Turbulence, Heat and Mass Transfer 10

On a checkerboard-free, conservative method for turbulent flows

J.A. Hopman*[,1], À. Alsalti-Baldellou[1,2], F.X. Trias[1] and J. Rigola[1]
[1]*Heat and Mass Transfer Technological Center, Technical University of Catalonia, ESEIAAT, c/Colom 11, 08222 Terrassa, Spain, jannes.hopman@upc.edu*
[2]*Termo Fluids SL, Sabadell (Barcelona), Spain; www.termofluids.com*

Abstract – This work investigates the checkerboard problem, a numerical artifact that arises in CFD simulations using collocated grid arrangements. The decoupling of odd and even cells leads to high frequency, non-physical pressure modes that lie on the kernel of the discrete Laplacian operator. To avoid this problem, a compact-stencil Laplacian is often used, but it introduces numerical dissipation, which disrupts the accurate capturing of the motion of fluids, especially at the smallest scales of turbulence. A better understanding of the origins of checkerboarding is sought after, using both wide and compact stencils, and three possible mechanisms for its occurrence are identified. Simple numerical tests are conducted to analyze these mechanisms, and more realistic simulations are used subsequently to verify the findings.

1. Introduction

Industrial CFD codes often make use of collocated grids. Consistently applying the central differencing scheme to discretise the Navier-Stokes equations in this arrangement leads to a wide-stencil Laplacian, in which odd and even cells are decoupled. This can result in high frequency, non-physical pressure modes, that lie on the kernel of the discrete Laplacian operator, commonly known as the checkerboard problem [2].

To avoid this problem and to decrease the computational complexity, a compact-stencil Laplacian is often applied, coupling neighbouring cells, at the cost of introducing numerical dissipation [6, 1]. This dissipation disrupts the accurate capturing of the motion of fluids, especially at the smallest scales of turbulence [8], and has been shown to be of a similar order of magnitude as applied LES models, decreasing their effectiveness [4].

Even with the use of compact stencils, the checkerboard problem has been observed, especially in unsteady cases using small timesteps [1]. In heat transfer problems, different timescales for momentum and thermal diffusivity can lead to this effect, allowing for oscillating pressure fields. Moreover, these patterns might arise through the wide-stencil velocity correction gradient. Therefore, using a compact-stencil Laplacian introduces numerical dissipation, especially affecting turbulence, without guaranteeing a solution to checkerboarding in all cases.

In this work, a better understanding of the origins of checkerboarding, using wide and compact stencils, is sought after. With this understanding, less dissipative solutions could become of interest, such as filtering the oscillatory pressure modes based on the kernel of the discrete Laplacian operator [5]. The existence and form of this kernel with respect to the mesh and discretisation method has been examined [3]. This work is extended by addressing the following questions: How does checkerboarding arise in the first place? And can it arise when the kernel of the discrete Laplacian only contains the constant mode?

To address these questions, a close examination of widely-used discretisations and algorithms was made and three possible mechanisms were identified. These mechanisms were analysed using simple numerical tests to gain a better understanding, and subsequently examined on more realistic, three-dimensional, turbulent cases.

Velocity predictor	$\mathbf{u}_c^p = \mathbf{u}_c^n - \Delta t \Omega^{-1} \left(C\left(\mathbf{u}_s^n\right) + D \right) \mathbf{u}_c^n$	(A1.1)
Poisson equation:		
if **wide** stencil $\rightarrow$	$L_c \tilde{\mathbf{p}}_c^{n+1} = M_c \mathbf{u}_c^p$	(A1.2a)
if **compact** stencil $\rightarrow$	$L \tilde{\mathbf{p}}_c^{n+1} = M_c \mathbf{u}_c^p$	(A1.2b)
Update cell-centered velocities	$\mathbf{u}_c^{n+1} = \mathbf{u}_c^p - G_c \tilde{\mathbf{p}}_c^{n+1}$	(A1.3)
Update face-centered velocities:		
if **wide** stencil: $\rightarrow$	$\mathbf{u}_s^{n+1} = \Gamma_{cs} \mathbf{u}_c^{n+1}$	(A1.4a)
if **compact** stencil: $\rightarrow$	$\mathbf{u}_s^{n+1} = \Gamma_{cs} \mathbf{u}_c^p - G \tilde{\mathbf{p}}_c^{n+1}$	(A1.4b)

Algorithm 1: Fractional step method for wide- and compact-stencil Laplacians

2. Possible causes of checkerboarding

The discrete Navier-Stokes equations were solved using the fractional step method. Algorithm 1 illustrates this method using Forward Euler time-integration, as an example. Following the notation of [7], $L_c = M_c G_c = M \Gamma_{cs} \Gamma_{sc} G$ is the so-called wide-stencil Laplacian operator and, if chosen consistently, the interpolators are related by:

$$\Gamma_{sc} = \Omega^{-1} \Gamma_{cs}^T \Omega_s. \tag{1}$$

This only leaves one degree of freedom, the choice of collocated-to-staggered interpolator, Γ_{cs}. Conversely, step (A1.2b) uses a compact-stencil Laplacian, $L = MG$. This eliminates the checkerboard problem at the cost of numerical dissipation related to non-zero divergence of the collocated velocities. Using this method, three different possible origins for the checkerboard problem were identified.

Mechanism 1
When using the compact-stencil method and letting $\Delta t \rightarrow 0^+$, the effect of the second term on the RHS of step (A1.1) diminishes until $\mathbf{u}_c^p = \mathbf{u}_c^n$. This situation leads to:

$$\mathbf{u}_c^n = \mathbf{u}_c^{n-1} - G_c \tilde{\mathbf{p}}_c^n = \mathbf{u}_c^0 - G_c \sum_i^n \tilde{\mathbf{p}}_c^i, \tag{2}$$

$$L \tilde{\mathbf{p}}_c^{n+1} = M_c \mathbf{u}_c^0 - L_c \sum_i^n \tilde{\mathbf{p}}_c^i, \tag{3}$$

$$L \hat{\mathbf{p}}_c^{n+1} = M_c \mathbf{u}_c^0 + \left(L \overset{i}{-} L_c \right) \hat{\mathbf{p}}_c^n, \tag{4}$$

in which $\hat{\mathbf{p}}_c^n = \sum_i^n \tilde{\mathbf{p}}_c^i$. This gives a solution to the equation in step (A1.2a) which can contain checkerboard modes that lie on the kernel of L_c, despite using a compact-stencil Laplacian. Moreover, the Rhie-Chow correction term may be too small when using a very small timestep to solve unsteady problems, leading to checkerboarding [2]. Low Prandtl number turbulent heat transfer problems may lead to such cases because of the disparity in thermal and momentum timescales. Additionally, steady-state solutions reached by transient solvers might lead to a similar effect, since the lack of change in the solution mimics the effect of very small timesteps.

Mechanism 2
The second method involves the choice of the Poisson solver. For a stationary iterative method the Poisson equation is solved by splitting the Laplacian operator, resulting in:

$$\tilde{\mathbf{p}}_c^{k+1} = R^{-1}M_c\mathbf{u}_c^p + R^{-1}S\tilde{\mathbf{p}}_c^k = \sum_{i=0}^{k}\left(R^{-1}S\right)^i R^{-1}M_c\mathbf{u}_c^p + \left(R^{-1}S\right)^{k+1}\tilde{\mathbf{p}}_c^0, \tag{5}$$

where L is split as $L = R - S$ and R is chosen to be easily invertible, e.g. $R = diag(L)$ for the Jacobi method. The second term on the RHS of equation (5) accounts for the initial guess and is optional. If the image of R^{-1}, $\mathrm{Im}\left(R^{-1}\right)$, is non-orthogonal to the kernel of L_c, $\mathrm{Ker}\left(L_c\right)$, the solution can contain checkerboard modes. These modes can subsequently be preserved by the initial guess. Similarly, if a preconditioner is used as:

$$Q_L^{-1}LQ_R^{-1}\tilde{\mathbf{q}}_c^{n+1} = Q_L^{-1}M_c\mathbf{u}_c^p, \tag{6}$$

where $Q_R^{-1}\tilde{\mathbf{q}}_c^{n+1} = \tilde{\mathbf{p}}_c^{n+1}$, then $\mathrm{Im}\left(Q_R^{-1}\right)$ might not be orthogonal to $\mathrm{Ker}\left(L_c\right)$, possibly leading to checkerboarding.

Mechanism 3
The third method involves the wide-stencil Laplacian that is implicitly formed by the divergence and gradient, M_c and G_c, on the RHS of the equations in steps (A1.2a), (A1.2b) and (A1.3). If both interpolations in these operators are consistent, e.g. both midpoint, we can show that this operation is symmetric:

$$M_cG_c = M\Gamma_{cs}\Gamma_{sc}G = M\Gamma_{sc}\Omega^{-1}\Gamma_{cs}^T\Omega_sG = -M\Gamma_{sc}\Omega^{-1}\Gamma_{cs}^TM^T, \tag{7}$$

where we used $G = -\Omega_s^{-1}M^T$ [7]. For symmetric matrices, the image and kernel are orthogonal, i.e. $L_c^T = L_c \Rightarrow \mathrm{Im}\left(L_c\right) \perp \mathrm{Ker}\left(L_c\right)$, if not, the result of this operation can contain checkerboard modes. This implicit M_cG_c occurs when rewriting the RHS of the equations in steps (A1.2a) and (A1.2b) using the equations in steps (A1.1) and (A1.3):

$$M_c\mathbf{u}_c^p = M_c\mathbf{u}_c^{p(n-1)} - M_cG_c\tilde{\mathbf{p}}_c^n - \Delta tM_c\Omega^{-1}\left(C\left(\mathbf{u}_s^n\right) + D\right)\mathbf{u}_c^n. \tag{8}$$

Therefore, checkerboarding might arise if the interpolators in G_c and M_c are chosen to be inconsistent with respect to each other, i.e. not according to equation (1).

3. Numerical results

Firstly, these methods are examined on a two-dimensional Taylor-Green vortex, monitoring the influence of several different parameters, such as kinematic viscosity (ν), Laplacian discretisation, mesh stretching and Poisson solver, see figure 1. Once better understood, the mechanisms and effects will be tested using a three-dimensional incompressible turbulent channel flow, see figure 2, and a differentially heated cavity (not shown). Using these more realistic and relevant cases, the presence and suppression of checkerboarding will be demonstrated, as well as the gain in accuracy when eliminating the numerical error introduced by the widely-used compact-stencil Laplacian.

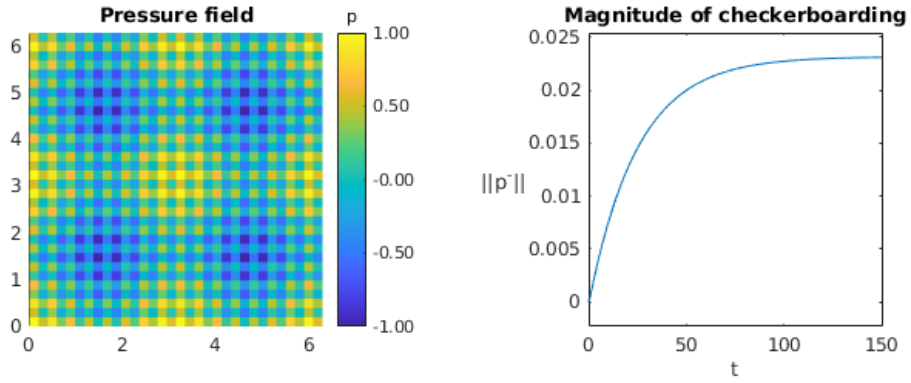

Figure 1: Visible checkerboard modes (p^-) in a Taylor-Green vortex using a uniform grid, $Re = 200\pi$, a PCG solver and incomplete Cholesky factorisation of the wide-stencil Laplacian

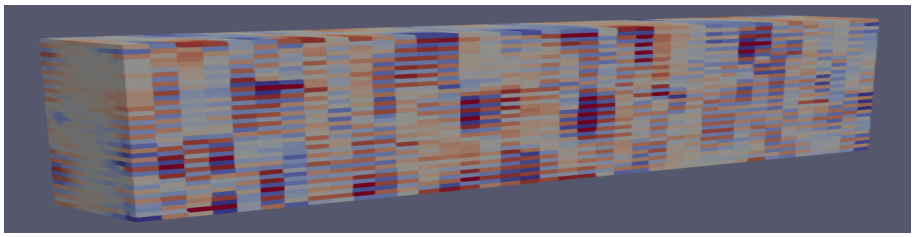

Figure 2: Checkerboarding in an incompressible turbulent channel flow at $Re_\tau = 180$

References

1. Felten, F. N., & Lund, T. S. (2006). Kinetic energy conservation issues associated with the collocated mesh scheme for incompressible flow. Journal of Computational Physics, 215(2), 465-484.
2. Ferziger, J. H., Perić, M., & Street, R. L. (2002). Computational methods for fluid dynamics (Vol. 3, pp. 196-200). Berlin: springer.
3. Hopman, J. A., Trias, F. X., Rigola, J. (2022). On a conservative solution to checkerboarding: Examining the discrete Laplacian kernel using mesh connectivity. Proceedings of the 13th International ERCOFTAC Workshop on Direct and Large-Eddy Simulation (DLES12), Held at the University of Udine, October 2022.
4. Komen, E. M., Hopman, J. A., Frederix, E. M. A., Trias, F. X., & Verstappen, R. W. (2021). A symmetry-preserving second-order time-accurate PISO-based method. Computers & Fluids, 225, 104979.
5. Larsson, J., & Iaccarino, G. (2010). A co-located incompressible Navier-Stokes solver with exact mass, momentum and kinetic energy conservation in the inviscid limit. Journal of Computational Physics, 229(12), 4425-4430.
6. Rhie, C. M., & Chow, W. L. (1983). Numerical study of the turbulent flow past an airfoil with trailing edge separation. AIAA journal, 21(11), 1525-1532.
7. Trias, F. X., Lehmkuhl, O., Oliva, A., Pérez-Segarra, C. D., & Verstappen, R. W. C. P. (2014). Symmetry-preserving discretization of Navier–Stokes equations on collocated unstructured grids. Journal of Computational Physics, 258, 246-267.
8. Verstappen, R. W. C. P., & Veldman, A. E. P. (2003). Symmetry-preserving discretization of turbulent flow. Journal of Computational Physics, 187(1), 343-368.